Nonadiabatic effects in the photoelectron spectra of HCl and DCl. II. Theory

L. Mauritz Andersson,[1,*] Florian Burmeister,[2] Hans O. Karlsson,[1] and Osvaldo Goscinski[1]
[1]*Department of Quantum Chemistry, Uppsala University, Box 518, SE-751 20 Uppsala, Sweden*
[2]*Department of Physics, Uppsala University, Box 530, SE-751 21 Uppsala, Sweden*
(Received 27 June 2001; published 12 December 2001)

The vibrationally resolved photoelectron spectra of HCl and DCl in the 25–28 eV region were computed using a time-dependent approach for the nuclear dynamics. The spectral features cannot be understood without including a nonadiabatic coupling between the dissociative $3\,^2\Sigma^+$ state and the bound $4\,^2\Sigma^+$ state in the adiabatic picture. Alternatively, in the diabatic picture a dissociative two-hole–one-particle state interacts with a bound one-hole state. The molecular system is of intermediate coupling strength, i.e., it cannot be described by a single potential-energy curve. The interaction between a bound and a dissociative state leads to Fano resonances superimposed on a broad background, as observed in the experimental spectra [Burmeister *et al.*, Phys. Rev. A **65**, 012704 (2001)]. From modified potential-energy curves, all features of the experimental spectra, including Fano resonance parameters and lifetimes, were reproduced. From the simulations we observe that two additional peaks in the experimental DCl spectra should appear if the resolution were to be enhanced to around 10 meV.

DOI: 10.1103/PhysRevA.65.012705 PACS number(s): 33.80.Eh, 31.50.Gh, 31.50.Df, 33.60.Cv

I. INTRODUCTION

The concept of potential energy curves (PEC) is central in chemical physics. It allows the description of chemical phenomena to take place on a single adiabatic curve, illustrating the making and breaking of bonds. The PEC are a consequence of the Born-Oppenheimer (BO) approximation, the decoupling of the nuclear and electronic degrees of freedom. The BO is normally assumed valid, at least in the region around the equilibrium. The BO approximation, together with the Franck-Condon approximation, has been successfully applied to a large range of molecular processes.

For a large class of photoinduced dynamics, the BO approximation is not valid. Several PEC, coupled by nonadiabatic couplings, must be considered. In this paper we will consider the photoelectron spectra of HCl/DCl in the 25–28 eV region, referring to recent experimental results by Burmeister *et al.* [1]. In their spectra interference phenomena and Fano-type resonances were observed, indicating a breakdown of the BO approximation. The structure of the spectra dictates that the system cannot be described by a single PEC in either the adiabatic or diabatic limit; it is an example of an intermediate coupling strength [2,3]. The appearance of Fano type resonances indicates a system with a bound state nonadiabatically coupled to a dissociative state.

The aim of this paper is to theoretically describe the experimental photoelectron spectra [1], identify the resonances, and determine the potential parameters. The computational model is described in Sec. II. Results are presented in Sec. III and summarized in Sec. IV.

II. THEORY

Within the Fermi Golden Rule approximation, the photoelectron spectra can be written as

$$S(E)\propto\langle\phi_g|\hat{\mu}\,\delta(E-\hat{H})\,\hat{\mu}|\phi_g\rangle=\langle\Psi|\,\delta(E-\hat{H})|\Psi\rangle. \tag{2.1}$$

Here $|\phi_g\rangle$ is the ground state and $\hat{\mu}$ the transition dipole operator. For the situation of interest here, the system is described by a two-state Hamiltonian in the diabatic representation

$$\hat{\mathbf{H}}=\hat{\mathbf{T}}+\hat{\mathbf{V}}=\frac{\hat{p}^2}{2\mu}1+\begin{pmatrix} U_b(\hat{r}) & U_{bd}(\hat{r}) \\ U_{bd}(\hat{r}) & U_d(\hat{r}) \end{pmatrix}. \tag{2.2}$$

The U_b is a bound and U_d a dissociative state of HCl^+, coupled via U_{bd}. The initial state $|\Psi\rangle$ is given by

$$|\Psi\rangle=\begin{pmatrix} |\psi_b\rangle \\ |\psi_d\rangle \end{pmatrix}=\begin{pmatrix} \mu_b|\phi_g\rangle \\ \mu_d|\phi_g\rangle \end{pmatrix}, \tag{2.3}$$

where μb and μd are transition dipole moments from the ground state The photoelectron spectra (2.1) can be computed in a time-dependent framework via a Fourier transform of the auto-correlation function [4]

$$S(E)\propto\frac{1}{\pi}\int_{-\infty}^{\infty}\langle\Psi|e^{-i\mathbf{H}t/\hbar}|\Psi\rangle e^{Et/\hbar}dt=\frac{1}{\pi}\int_{-\infty}^{\infty}C(t)e^{Et/\hbar}dt. \tag{2.4}$$

To propagate the wave function, the split-operator (SO) method [5] with pseudospectral (fast Fourier transform) evaluation of space derivatives was used. The method is second order in time and has spectral accuracy in space. The quantum state $|\Psi\rangle$ was propagated up to a time T, which, using that $C(-t)=C^*(t)$, gives the correlation function in the interval $[-T,T]$. The integral in Eq. (2.4), giving the photoelectron spectra, was computed via the fast Fourier transform combined with a Hanning window. The resolution is determined by the length of the propagation T, e.g., a spectral resolution of 4 meV was gained after $T=500$ fs.

*Corresponding author.
Email address: mauritz.andersson@kvac.uu.se

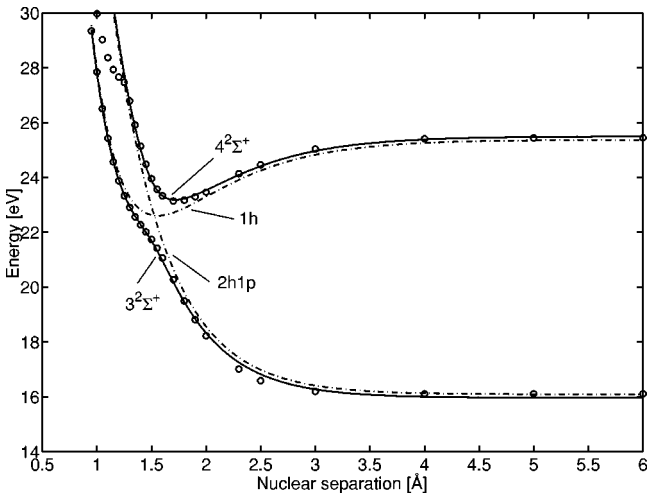

FIG. 1. Adiabatic potential energy curves for HCl^+ and DCl^+ $3^2\Sigma^+$ and $4^2\Sigma^+$, according to Hiyama and Iwata [6], shown with circles. The fitted diabatic curves with resulting adiabatic curves are also shown (dashed and solid lines, respectively). Energies are relative to the dissociation limit for the neutral ground state. To relate to the photoelectron spectra, add the neutral ground state dissociation energy, $D_0 = 4.04$ eV for HCl [6]

TABLE I. Diabatic potential parameters for HCl^+ and DCl^+ fitted to the adiabatic curves [6] for the $3^2\Sigma^+$ and $4^2\Sigma^+$ states. Energies are relative to the dissociation limit for the neutral ground state. According to Hiyama and Iwata [6], $D_0 = 4.04$ eV for the neutral HCl ground state.

Parameter	Value (au)	Comment
α_b	0.8272	
T_b	0.8306	
r_b	2.942	
D_b	0.1019	
α_d	1.0778	
T_d	0.5912	
r_d	0	
D_d	5.3456	related to the choice of r_d
U_{bd}	0.0400	R independent

III. RESULTS

Accurate potential energy curves, with nonadiabatic couplings, are needed to describe the dynamics. Adiabatic PEC for HCl^+ have been computed by Hiyama and Iwata [6]. In the energy region of interest here, 25–28 eV, the $3\,^2\Sigma^+$ and $4\,^2\Sigma^+$ adiabatic states are the only candidates, exhibiting an avoided crossing between a bound and a dissociative state. As discussed in Ref. [6], the ground state of HCl has the dominant configuration $(4\sigma)^2(5\sigma)^2(2\pi)^4(6\sigma)^0$ with corrections, especially at large distances, by the pair excitation $(4\sigma)^2(5\sigma)^0(2\pi)^4(6\sigma)^2$. This, in principle, allows for excitation to the two-hole–one-particle state $4\,^2\Sigma^+$, but this has a very small contribution (see below). At long bond distances the $3\,^2\Sigma^+$ state has the electronic configuration $(4\sigma)^2(5\sigma)^0(2\pi)^4(6\sigma)^1$, which has two-hole–one-particle character. To the left of the crossing, the configuration is mostly $(4\sigma)^1(5\sigma)^2(2\pi)^4(6\sigma)^0$, which implies a large photoionization cross section since it is a one-hole state. The $4\,^2\Sigma^+$ state has at long distances the same one-hole configuration. At small r, inside the avoided crossing the configuration is changed to the same two-hole–one-particle character as $3\,^2\Sigma^+$ has for long r.

Thus the system can be described as an interaction between two diabatic states, one bound of two-hole–one-particle character and one dissociative of one-particle character. The nonadiabatic coupling is a sharply peaked function of derivatives of the nuclear coordinate in the adiabatic picture. In the diabatic picture, which is used here, it is a smooth potential function and thus easier to include in computational models. The two pictures describe the same physics and it is always possible to transform between the two representations for a one-dimensional problem via an r-dependent rotation of the electronic states [7].

The adiabatic PEC of Hiyama and Iwata [6] are given as a set of *ab initio* points. There is no information on the

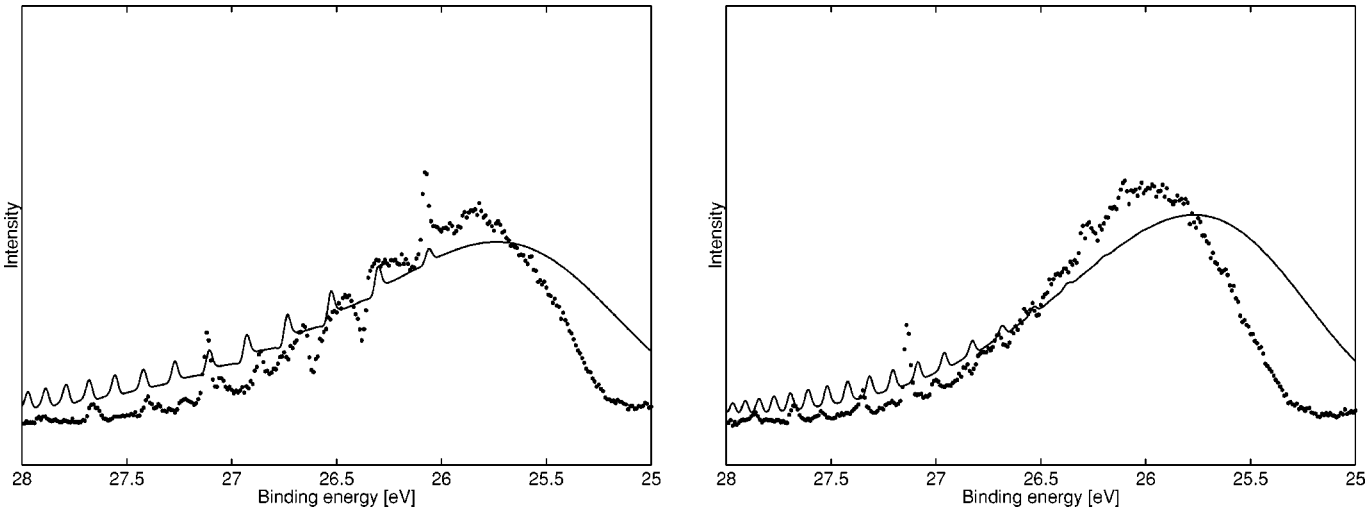

FIG. 2. Photoelectron spectra for HCl (top) and DCl (bottom) using potentials in Fig. 1, Table I. The resulting theoretical spectra were down-shifted in energy with the arbitrary value of 1.3 eV.

adiabatic couplings. To transform to the diabatic basis we have to assume the form of the diabatic states and the coupling. For the bound state, a Morse potential

$$U_b(r) = D_b(1 - e^{\alpha_b(r-r_b)})^2 + T_b \tag{3.1}$$

was used and for the dissociative state an exponential form

$$U_d(r) = D_d e^{-2\alpha_d(r-r_d)} + T_d \tag{3.2}$$

was used. The coupling U_{bd} was assumed to be constant (a Gaussian form was also tested with no significant difference). This choice can be justified since the crossing between the two U_b and U_d states is localized. The potential and coupling parameters were computed by diagonalizing the 2×2 potential matrix and fitting the resulting adiabatic curves to the *ab initio* curves by Hiyama and Iwata [6]. The resulting curves are shown in Fig. 1 and the parameters are given in Table I. The energies are given relative to the dissociation limit of the electronic ground state of the neutral molecule to be independent of deuteration.

For the neutral ground state of HCl the experimental dissociation energy (D_0) is 4.43 eV and for DCl $D_0 = 4.48$ eV, values that were used as an energy reference in the resulting spectra. The initial state $|\phi_g\rangle$ was computed using the Morse ground-state potential parameters $\omega_e = 0.0136$ a.u., $x_e\omega_e = 0.000\,240\,6$ a.u., and $r_e = 2.4086$ a.u. [8]. This gives $D_e = 0.18905$ au and $\alpha_e = 0.64376$ au. These Morse parameters give $D_0 = 4.96$ eV for HCl, which conflicts with the above experimental value. Here the experimental dissociation energy was used for the energy reference, and the above Morse parameters were used for computing the initial state.

From the diabatic curves, extracted from Ref. [6], the photoelectron spectra for HCl and DCl were computed using the time-dependent wave-packet approach. The result is depicted in Fig. 2. To match the first resonance peaks of the experimental cross section for HCl the spectra had to be shifted down with an energy of 1.3 eV. In the experimental spectra a number of features can be seen. A broad continuum envelope with a vibrational progression, denoted A, on top shows distinct Fano interference profiles, notably more distinct in HCl than in DCl. A second progression, denoted B, is also seen starting above 27 eV. As can be seen in the theoretical spectra, the discrete peaks for HCl are very much subdued compared to the experimental spectrum. This indicates that the *ab initio* computations overestimate the avoided crossing. The vibrational peaks in the theoretical spectrum are less separated compared with experiment, indicating an underestimation of the bonding stiffness. The continuum envelope is broader than in the experiment for both HCl an DCl. Although the overall picture is remarkably consistent with experiment the details differ. From this we draw the conclusion that the PEC are not accurate enough, as already discussed for these highly excited states by Hiyama and Iwata [6].

To improve the potential energy curves, we optimized the potential parameters via a fitting of the computed spectra to the experiment. The number of independent parameters can be reduced as follows. The dissociation limits for the $3\,^2\Sigma^+$ and $4\,^2\Sigma^+$ states are known from experimental data [8,9] on Cl and Cl^+. The $3\,^2\Sigma^+$ state correlates with $H(1s;\,^2S)$, $Cl^+(1s^1 3p^5;\,^3P, J=0)$ and the $4\,^2\Sigma^+$ correlates with $H(1s;\,^2S)$, $Cl^+(1s^2 3p^4;\,^1S)$. The ionization energy of Cl is 12.967 64 eV ($^3P;J=2$) and from there the excitation energy to $Cl^+(1s^2 3p^4;\,^1S)$ is 3.456 435 eV and to $Cl^+(1s^1 3p^5;\,^3P, J=0)$ is 11.695 91 eV. Together this gives $T_d = 16.424$ eV and $T_b + D_b = 24.664$ eV relative to the dissociation limit for the neutral molecular ground state. To get a reasonable behavior for small r we chose to set α_d equal to α_b. These constraints lead to five independent parameters $(\alpha_b, r_b, D_b, r_d, U_{bd})$ describing the potentials and the coupling.

TABLE II. Predicted diabatic potential parameters for HCl^+ and DCl^+. The resulting adiabatic states corresponds to the $3^2\Sigma^+$ and $4^2\Sigma^+$ states. The independent parameters were determined by fitting HCl theoretical photoelectron spectra to experiment. All energies are relative to the dissociation limit for the neutral ground state. See text for details.

Parameter	Value (au)	Comment
α_b	0.6972	
T_b	0.77262	from atomic Cl excitation
r_b	2.908	
D_b	0.13378	
α_d	0.6972	same as α_b
T_d	0.60357	from atomic Cl excitation
r_d	3.039	
D_d	0.16903	determined by r_d
U_{bd}	0.02540	R independent

The parameters were optimized using a multidimensional unconstrained nonlinear minimization in the energy range 25.2 eV–27.07 eV. The fitted parameters are given in Table

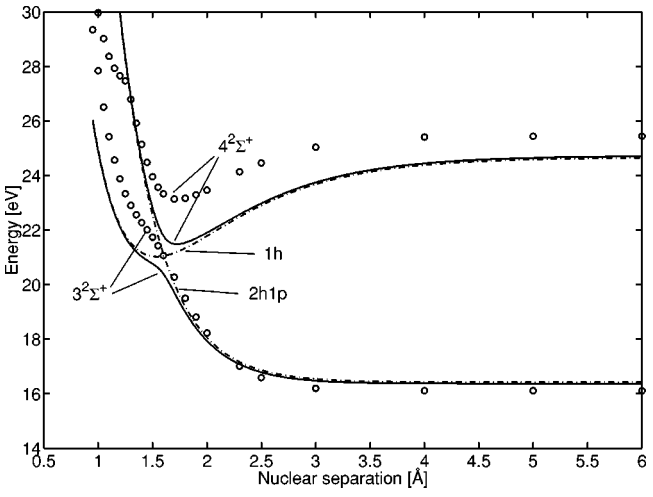

FIG. 3. Proposed diabatic (dashed) and adiabatic (solid) curves from this work. Adiabatic potential energy curves according to Hiyama and Iwata [6] are shown as circles. Energies are relative to the dissociation limit for the neutral ground state. $D_0 = 4.43$ eV for HCl and $D_0 = 4.48$ eV for DCl. The parameters can be found in Table II.

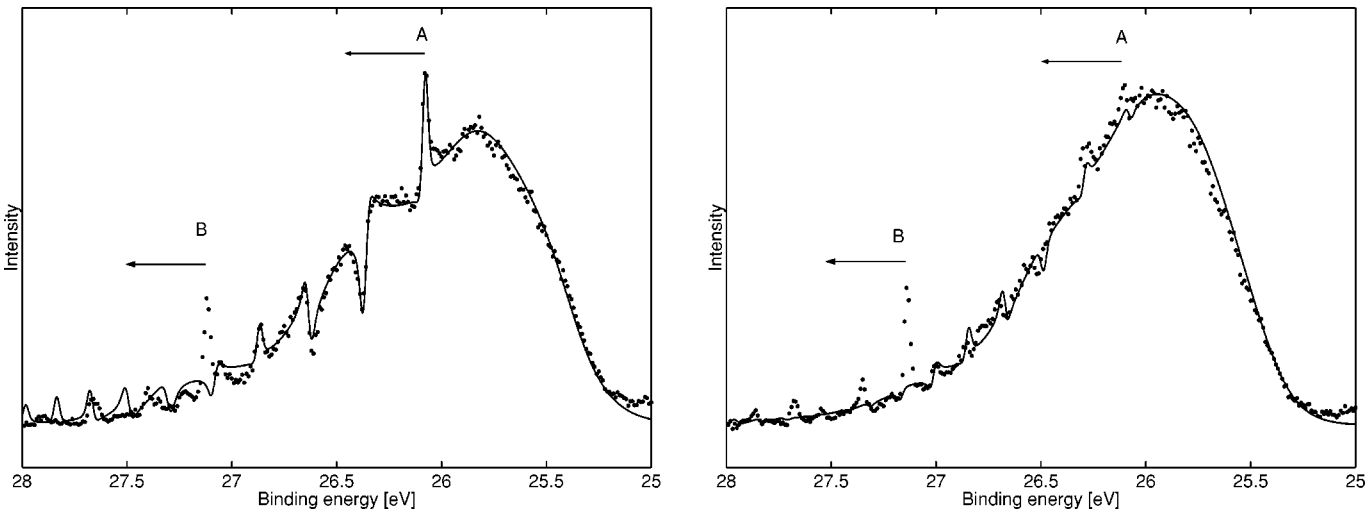

FIG. 4. Photoelectron spectra for HCl (top) and DCl (bottom) using proposed potentials in Fig. 3, Table II. The five parameters were obtained from fitting to the experimental HCl spectra in a least squares sense over the range 25.2–27.07 eV. The same parameters were then used to obtain the DCl spectra. No arbitrary shifting was performed in either case. Note the narrower overall envelope in the DCl case, which is due to a more localized initial state.

II and the resulting potential curves in Fig. 3. Above 27.07 eV the second vibrational progression (B) starts to influence the spectra and the minimization process would be disturbed if this region were included. The B progression is not included in the theoretical model. As was discussed in the experimental paper, it is probably due to a $(4\sigma)^2(5\sigma)^2(2\pi)^2(1\delta)^1$ state. To our knowledge there is no PEC available for this state. We will return to this vibrational progression in future work. It can also not be ruled out that the state responsible for the B progression may be disturbing the intensity of the A progression in the high-energy range.

The photoelectron spectra computed from the optimized curves, Fig. 3, is shown together with experimental points in Fig. 4, convoluted with a Gaussian of full width at half maximum=30 meV. All features of the experimental spectrum for both HCl and DCl are reproduced in the theoretical spectrum (except for the B progression as discussed above). This includes the overall position of the band, the detailed shape of the continuum and the position, shape and intensity of the five (six) lowest peaks in HCl (DCl).

The coupling between a bound and a dissociative state gives rise to Fano resonances [10] with the resonance contribution to the spectra given by

$$S_{res} \propto \frac{(\epsilon+q)^2}{1+\epsilon^2}, \tag{3.3}$$

where $\epsilon=2(E-E_r)/\Gamma$ is a dimensionless reduced energy. The resonances can thus be characterized by three parameters: position E_r, lifetime $\tau=2/\Gamma$, and the Fano parameter q. From a time-independent approach, based on pseudospectral discretization and smooth-exterior scaling [11–13], E_r, τ, and q were computed for the first few resonances, as shown in Tables III and IV. In [1] Burmeister *et al.* noted that the peaks for DCl below 27 eV almost disappear. From the results shown here it is clear that this is due to limited experimental resolution combined with lower resonance intensity. In Fig. 5 the unconvoluted theoretical spectra are shown. Together with Table IV it can be seen that the peaks for DCl are there, but they are much sharper than the corresponding peaks for HCl. In fact, there are two peaks that are not resolved experimentally. By increasing the experimental resolution to around 10 meV it should be possible to detect the DCl peaks also.

To test the model and its sensitivity to the actual values of the parameters, we first changed the HCl $D_0=4.43$ eV of the ground state to $D_0=4.96$ eV (from the experimental Morse parameters, as discussed above), and the potential parameters were reoptimized. The resulting photoelectron spectrum did not change significantly, with potentials very similar in the energy region of the spectrum. Second, the α_d was varied $\pm 20\%$ compared to α_b, and again the potential and spectra did not change. The proposed potentials are thus robust in the energy range of interest.

TABLE III. The first five Fano resonances for HCl^+.

Position [eV]	Lifetime [ps]	q
26.0794	2.6875	−6.202
26.3663	0.0528	−0.3899
26.6335	0.1019	0.9305
26.8687	2.7199	−6.3277
27.0864	0.0594	−0.5323

TABLE IV. The first six Fano resonances for DCl^+.

Position [eV]	Lifetime [ps]	q
26.0793	1.2800	0.81348
26.2904	1.767	−1.9125
26.4879	0.1944	0.10429
26.6741	0.4495	1.7768
26.8468	2.5226	−5.5988
27.0107	0.1523	−1.027

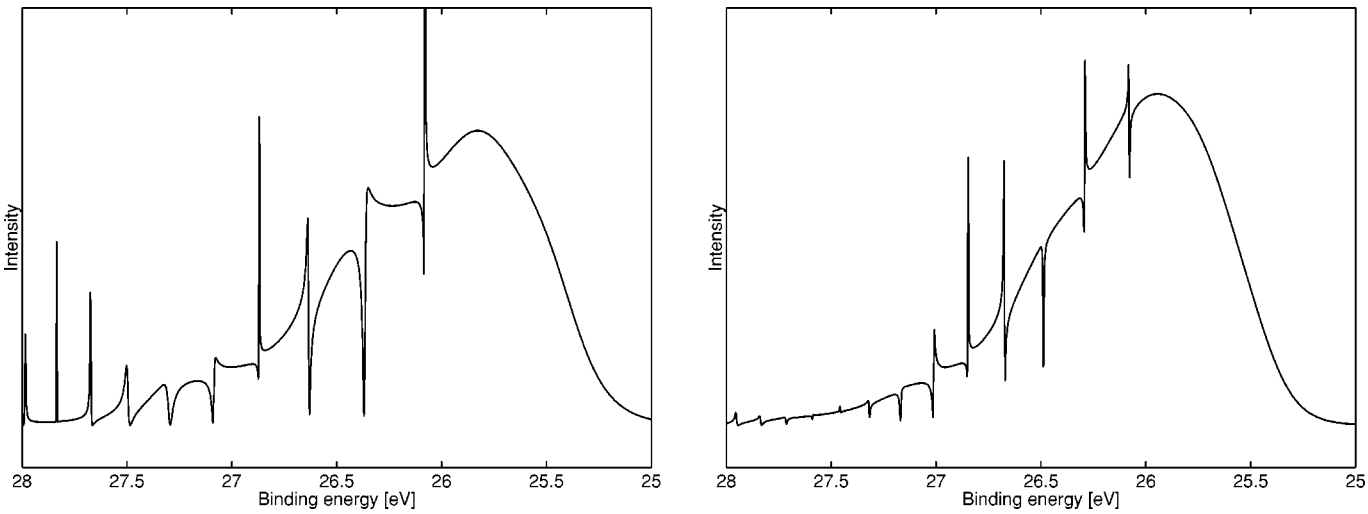

FIG. 5. To illustrate the Fano profiles we show the theoretical unconvoluted photoelectron spectra for HCl (top) and DCl (bottom) obtained from the potentials in Fig. 3, Table II.

It is important to realize that the nonadiabatic coupling is of intermediate strength, i.e., the system cannot be described as taking place on a single PEC in either the adiabatic or the diabatic representation. To illustrate this, the time dependence of the nuclear probability density $|\Psi(r,t)^2|$ in the two representations is shown in Figs. 6 and 7. If the adiabatic picture were preferred we would see a dissociating wave packet in the dissociative state and vibrations in the bound state. As is seen, this is not the case either for HCl or for DCl. The same is true if we take the diabatic view, hence it is *not* possible to understand the dynamics as taking place on a single potential curve. However, it can be seen that the probability of transition between the adiabatic states is lower for DCl than for HCl. This is consistent with the lower speed of the wave packet traversing the avoided crossing, as can be seen in the figure.

The details of the photoelectron spectra are sensitive to the the values of the electronic dipole transition moments μ_b and μ_d, which enter into Eq. (2.3). Without explicit knowledge of their actual value and shape, is not clear how much weight should be given to each (diabatic) state in the simulations. Here we made the assumption that the (diabatic) one-hole state $|\phi_b\rangle$ is the only one with a transition dipole moment different from zero. This means that photoexcitation takes place to the diabatic state. Excitation to the dissociative *adiabatic* state instead gave only small changes in spectra, with the exception of increased (approximately doubled) intensity in the peaks above 27.3 eV. The intensity in these peaks was too large even when using the diabatic excitation. Thus we argue that the diabatic picture is the preferred one to describe the excitation process, which can be understood since the transition dipole moment is more constant in the

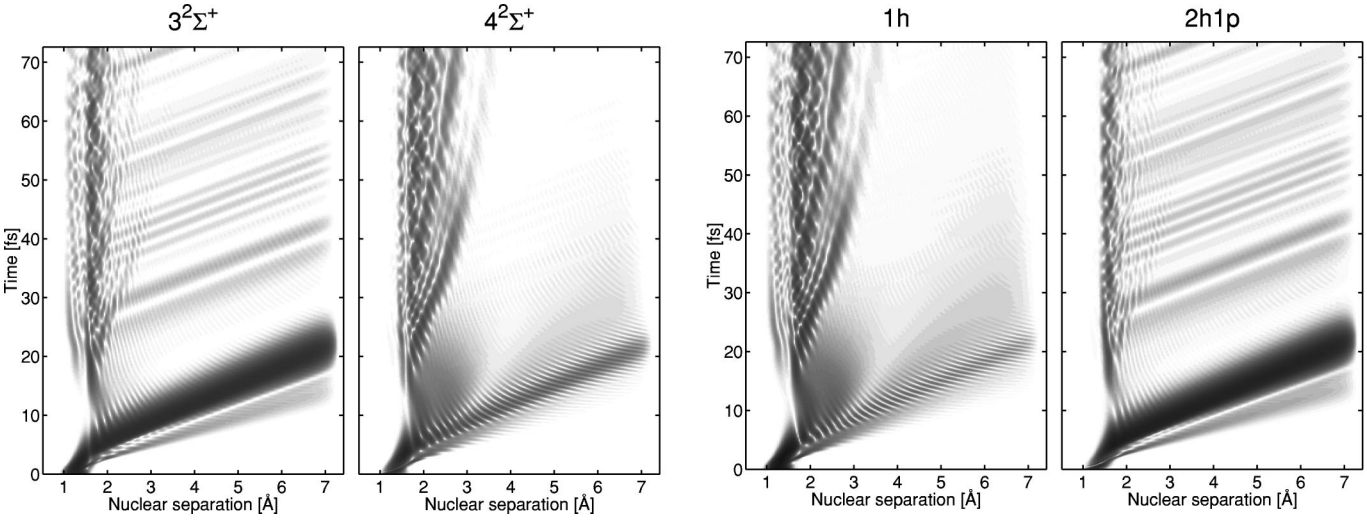

FIG. 6. Time dependence of the nuclear density in HCl projected to the adiabatic picture (left) and the diabatic picture (right). The left panels show the state that is lowest in energy at the inner positions, i.e., dissociative adiabat ($3^2\Sigma^+$) and bound diabat (1h). The right panels show the bound adiabat ($4^2\Sigma^+$) and dissociative diabat (2h1p). What is notable is that neither the adiabatic nor the diabatic picture is preferred for interpretation. We see clear effects of an intermediate coupling strength.

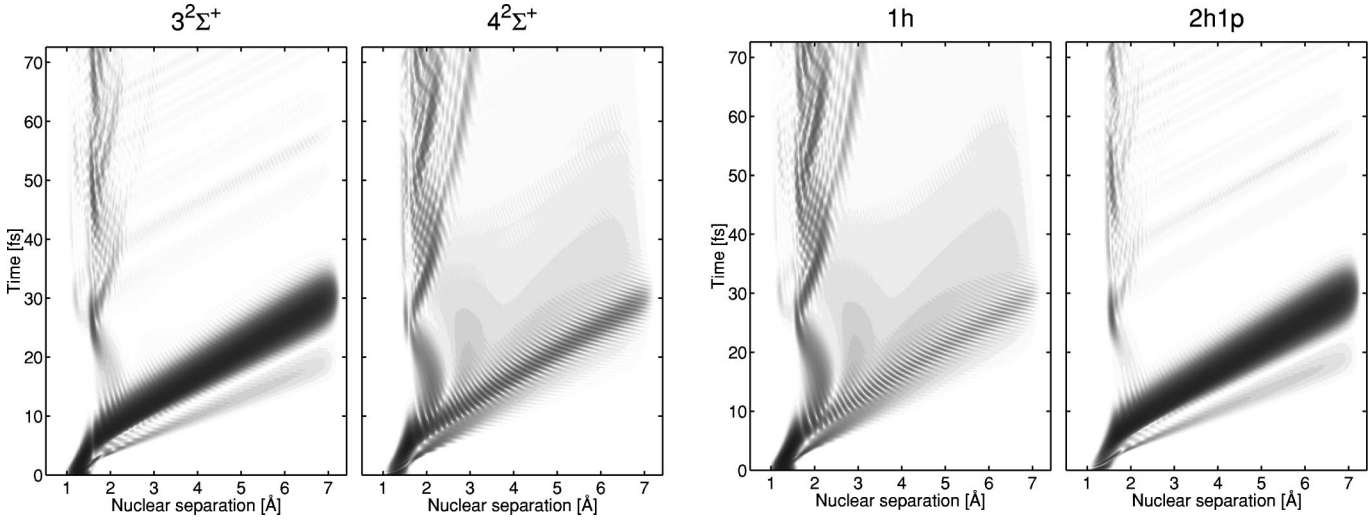

FIG. 7. Time dependence of the nuclear density in DCl projected to the adiabatic picture (left) and the diabatic picture (right). The left panels show the state that is lowest in energy at the inner positions, i.e., dissociative adiabat ($3^2\Sigma^+$) and bound diabat (1h). The right panels show the bound adiabat ($4^2\Sigma^+$) and dissociative diabat (2h1p). Note the slower dissociation speed and the decreased nonadiabatic transfer compared to HCl.

diabatic than in the adiabatic picture. Assuming the transition dipole moment for the two-hole–one-particle state to be nonzero increases this erroneous intensity even more, hence we conclude that the transition dipole moment to the two-hole–one-particle state is near zero. (Although the ground state had, according to Hiyama and Iwata [6], some pair excitation character, this must be negligible in the Frank-Condon region.). The assumed constant coupling is probably responsible for giving intensity to the high energy peaks and they might be suppressed in a more localized coupling model.

IV. SUMMARY

Complicated resonance patterns in spectra of photoinduced processes is an indication of the breakdown of the Born-Oppenheimer approximation. Nonadiabatic couplings between several electronic states must be included in a model of the molecular system. These couplings are nontrivial to compute and are often approximated with a constant value.

In this paper we have computed the photoelectron spectra for HCl and DCl. We have reproduced and explained all the features seen in the experiments [1]. By computing Fano resonance positions, lifetimes, and q values, we showed that by increasing the experimental resolution to about 10 meV two further peaks in the DCl spectrum should be visible.

To have an accurate comparison with experiment, high accuracy potential energy curves are needed. For HCl^+, high- level electronic structure theory did not yield accurate enough curves. Based on the assumption of an interaction between a (diabatic) bound and a dissociative state, improved PEC was constructed, optimized with respect to the experimental spectra.

ACKNOWLEDGMENTS

The authors would like to thank Miyabi Hiyama for sending the potential data from Ref. [6]. H.O.K. and O.G. would like to acknowledge financial support from the Swedish Research Council.

[1] F. Burmeister *et al.*, Phys. Rev. A **65**, 012704 (2001).
[2] M. Child, Mol. Phys. **32**, 1495 (1976).
[3] W. Qin, D. McCoy, L. Torop, and A. Blake, Chem. Phys. **221**, 77 (1997).
[4] E. Heller, Acc. Chem. Res. **14**, 368 (1981).
[5] M. Feit, J. F. Jr, and A. Steiger, J. Comput. Phys. **47**, 412 (1982).
[6] M. Hiyama and S. Iwata, Chem. Phys. Lett. **210**, 187 (1993).
[7] C. Mead and D. Truhlar, J. Chem. Phys. **84**, 1055 (1986).
[8] K. Huber and G. Herzberg, in *NIST Chemistry WebBook, NIST Standard Reference Database Number 69*, edited by W. Mallard and P. Linstrom (National Institute of Standards and Technology, Gaithersburg, 2000).
[9] R. Kelly, J. Phys. Chem. Ref. Data Suppl. **16**, 1 (1987).
[10] U. Fano, Phys. Rev. **124**, 1866 (1961).
[11] H. Karlsson, J. Chem. Phys. **108**, 3849 (1998).
[12] H. Karlsson, J. Chem. Phys. **109**, 9366 (1998).
[13] H. Karlsson, Eur. Phys. J. D **11**, 207 (2000).